

Geometric approach to the accuracy analysis of a class of 3-DOF planar parallel robots

Alexander Yu ^a, Ilian A. Bonev ^{b,*}, Paul Zsombor-Murray ^a

^a *Department of Mechanical Engineering, McGill University, 817 Sherbrooke St.W., Montreal, Canada H3A 2K6*

^b *Department of Automated Manufacturing Engineering, École de technologie supérieure (ÉTS),
1100 Notre-Dame St.W., Montreal, Quebec, Canada H3C 1K3*

Received 12 June 2006; received in revised form 11 December 2006; accepted 16 March 2007
Available online 3 May 2007

Abstract

Parallel robots are increasingly being used in industry for precise positioning and alignment. They have the advantage of being rigid, quick, and accurate. With their increasing use comes a need to develop a methodology to compare different parallel robot designs. However no simple method exists to adequately compare the accuracy of parallel robots. Certain indices have been used in the past such as dexterity, manipulability and global conditioning index, but none of them works perfectly when a robot has translational and rotational degrees of freedom. In a direct response to these problems, this paper presents a simple geometric approach to computing the exact local maximum position error and local maximum orientation error, given actuator inaccuracies. This approach works for a class of three-degree-of-freedom planar fully-parallel robots whose maximal workspace is bounded by circular arcs and line segments and is free of singularities. The approach is illustrated on three particular designs.

© 2007 Elsevier Ltd. All rights reserved.

Keywords: Parallel robots; Dexterity map; Workspace; Positioning; Accuracy; Error analysis

1. Introduction

Parallel robots which were once constructed solely in academic laboratories have increasingly been used in industry for positioning and alignment in recent years. With such demand in the market today for these fast and agile machines, new parallel robots are being designed and manufactured. However, there are still many key issues regarding the design of new parallel robots, such as optimal design and performance indices. How could one prove that a new parallel robot design is an improvement over existing designs? Is it enough to evaluate a robot based on its workspace? Clearly in the current industrial climate it is not, as positioning accuracy has become a key issue in many applications.

* Corresponding author.

E-mail address: ilian.bonev@etsmtl.ca (I.A. Bonev).

Several well defined performance indices have been developed extensively and applied to serial and parallel robots. However, a recent study [1] reviewed these indices and discussed their severe inconsistencies when applied to parallel robots with translational and rotational degrees of freedom. The study reviewed the most common indices to optimize parallel robots: the dexterity index [2], the various condition numbers applied to it to increase its accuracy such as the two-norm or the Frobenius number, and the global conditioning index that is computed over the complete workspace of the robot [3]. The conclusion of the paper is that these indices should not be used for parallel robots with mixed types of degrees of freedom (translations and rotations).

When the authors designed a new three-degree-of-freedom (3-DOF) planar parallel robot, they compared it to a similar design using the dexterity index [4]. This comparison was somewhat fair, because the designs allow the use of identical dimensions. However should one change the magnitude of the units (e.g., from cm to mm), the numbers within the index would change dramatically. The higher value for the length units would essentially make the dexterity of a robot closer to 0 as shown in Fig. 1.

The dexterity indices are very sensitive to both the type of units used and their magnitudes because of the dependence on the Jacobian matrix. This matrix also mixes non-invariant functions such as translational and rotational capabilities. A possible solution to this problem is the addition of condition numbers, however with each condition number there are particular problems as described in [1].

The global conditioning index (GCI) can be used to evaluate a robot over its workspace, which can be used for the optimal design of a robot. However, there remain two problems with this index. Firstly, it is still dependant on a condition number whose problems were outlined in [1]. Secondly, it is computationally-intensive.

Obviously, the best accuracy measure for industrial parallel robots would be the local maximum position error and local maximum orientation error, given actuator inaccuracies (input errors), or some generalization of this (e.g., mean value and variance of the errors over a specific workspace). A general method that can be used for calculating these errors based on interval analysis was proposed recently in [5]. However, this method is computationally-intensive and gives no kinematic insight into the problem of optimal design.

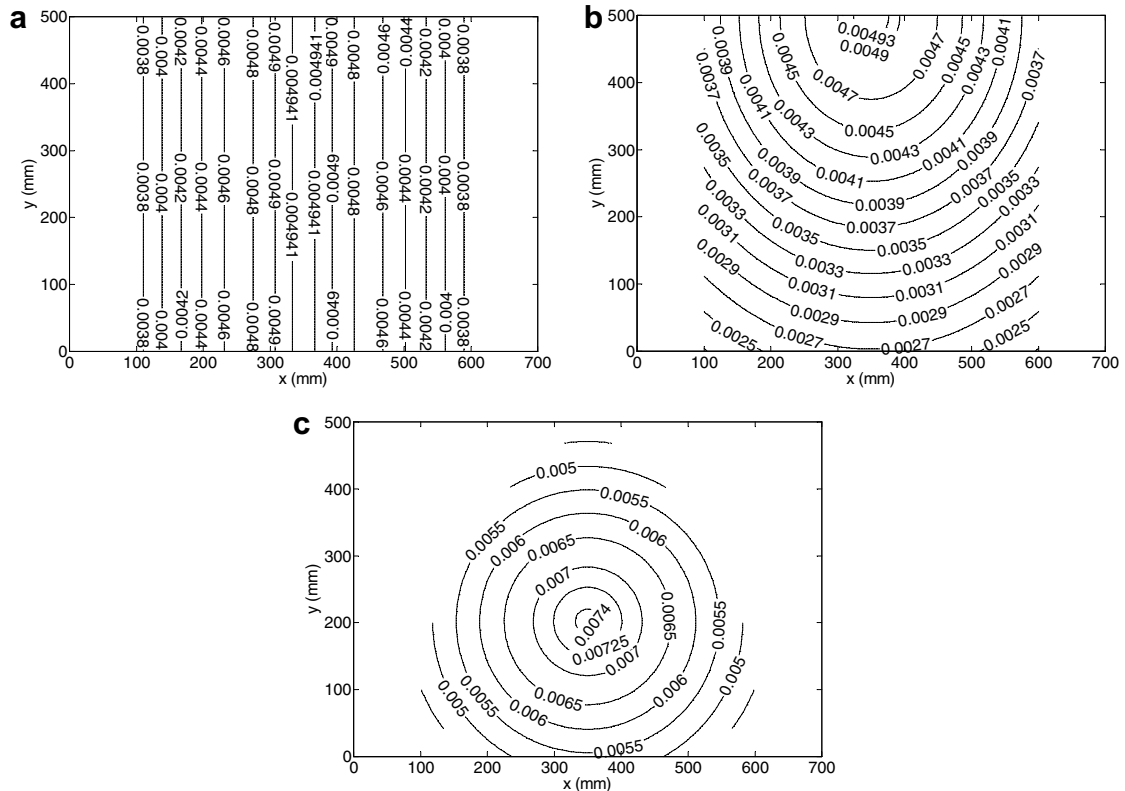


Fig. 1. Example of dexterity maps for (a) PreXYT, (b) Hephaist's parallel robot and (c) the Star-Triangle parallel robot.

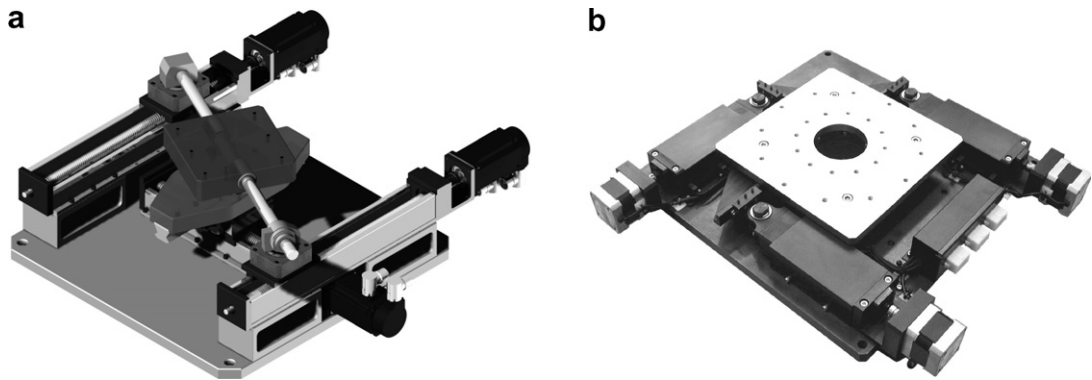


Fig. 2. (a) PreXYT (patent pending) and (b) Hephaist's NAF3 alignment stage (courtesy of Hephaist Seiko Co., Ltd).

In contrast, this paper presents a simple geometric approach for computing the exact local maximum position error and local maximum orientation error for a class of 3-DOF planar fully-parallel robots, whose maximal workspace is bounded by circular arcs and line segments and is free of singularities. The proposed approach is not only faster than any other method (for the particular class of parallel robots) but also brings valuable kinematic insight.

The approach is illustrated on three particular designs that are arguable among the best candidates for micro-positioning over a relatively large workspace:

1. A new parallel robot, named PreXYT, designed and constructed at École de technologie supérieure (ÉTS) that has a unique $2\text{-}\underline{PRP}/1\text{-}\underline{PPR}$ configuration (P and R stand for passive prismatic and revolute joints, respectively, while \underline{P} stands for an actuated prismatic joint). A CAD model of PreXYT is shown in Fig. 2a.
2. Hephaist's $3\text{-}\underline{PRP}$ parallel robot, designed by the Japanese company Hephaist Seiko and currently in commercial use. A photo of the industrial model is shown in Fig. 2b.
3. Star-Triangle parallel robot, another $3\text{-}\underline{PRP}$ parallel robot designed at LIRMM in France [6]. This robot is a more optimal design of the double-triangular parallel manipulator [7].

The remainder of this paper is organized as follows. The next section presents the proposed geometric approach. Then, Section 3 presents the inverse and direct kinematic equations for all three parallel robots whose accuracy will be studied in this paper. Section 4 briefly describes the geometry of the constant-orientation workspace for each of the three robots. Finally, Section 5 applies the proposed geometric method for computing the local maximum position and orientation errors. Conclusions are given in the last section.

2. Geometric method for computing output errors

Consider a 3-DOF fully-parallel planar robot at a desired (nominal) configuration. Let x , y , and ϕ denote the nominal position and nominal orientation of the mobile platform and ρ_1 , ρ_2 , and ρ_3 denote the nominal active-joint variables. Due to actuator inaccuracies of up to $\pm\epsilon$, the actual active-joint variables are somewhere in the ranges $[\rho_i - \epsilon, \rho_i + \epsilon]$ ($i = 1, 2, 3$). Therefore, the actual position and orientation of the mobile platform are $x + \Delta x$, $y + \Delta y$, and $\phi + \Delta\phi$, respectively. The question is, given the nominal configuration of the robot $(x, y, \phi, \rho_1, \rho_2, \rho_3)$ and the actuator inaccuracy $\pm\epsilon$, how much is the *maximum position error*, i.e., $\delta_{\max} = \max(\sqrt{\Delta x^2 + \Delta y^2})$, and the *maximum orientation error*, i.e., $\sigma_{\max} = \max(|\Delta\phi|)$.

In order to compute these errors, we basically need to find the values of the active-joint variables for which these errors occur. The greatest mistake would be to assume that whatever the robot and its nominal configuration, the maximum position error occurs when each of the active-joint variables is subjected to a maximum input error, i.e., $+\epsilon$ or $-\epsilon$. Indeed, in [8], it was proven algebraically that the maximum orientation angle of a 3-DOF planar parallel robot may occur at a Type 1 (serial) or a Type 2 (parallel) singularity, or when two leg wrenches are parallel, for active-joint variables that are inside the input error intervals. Similarly, it was pro-

ven that not all active-joint variables need to be at the limits of their input error intervals for a maximum position error.

Naturally, though there are exceptions, 3-DOF planar parallel robots that are used for precision positioning operate far from Type 1 singularities and certainly far from Type 2 singularities (if such even exist). Furthermore, it is simple to determine whether configurations for which two leg wrenches are parallel correspond to a local maximum of the orientation error and to design the robot in such a way that no such configurations exist. Therefore, for such practical 3-DOF planar parallel robot, the local maximum orientation error occurs at one of the eight combinations of active-joint variables with $+\varepsilon$ or $-\varepsilon$ input errors.

Now, finding this local maximum position error is equivalent to finding the point from the uncertainty zone of the platform center that is farthest from the nominal position of the mobile platform. This uncertainty zone is basically the maximal workspace of the robot obtained by sweeping the active-joint variables in the set of intervals $[\rho_i - \varepsilon, \rho_i + \varepsilon]$. Obviously, the point that we are looking for will be on the boundary of the maximal workspace.

A geometric algorithm for computing this boundary is presented in [9], but we will not discuss it here in detail. We need only mention that this boundary is composed of segments of curves that correspond to configurations in which at least one leg is at a Type 1 singularity (which we exclude from our study) or at an active-joint limit. When these curves are line segments or circular arcs, it will be very simple to find the point that is farthest from the nominal position of the mobile platform. This point will be generally an intersection point on the boundary of the maximal workspace.

In what follows, three examples will be studied in order to illustrate the proposed geometric approach.

3. Inverse and direct kinematic analysis

Referring to Fig. 3a–c, a base reference frame Oxy is fixed to the ground and defines a plane of motion for each planar parallel robot. Similarly, a mobile reference frame $Cx'y'$ is fixed to the mobile platform and in the same plane as Oxy . Let A_i be a point on the axis of the revolute joint of leg i (in this paper, $i = 1, 2, 3$) and in the plane of Oxy .

Referring to Fig. 3a and b, the base y -axis is chosen along the path of motion of point A_2 , while the mobile x' -axis is chosen along the line A_2A_3 . In Fig. 3a, the origin C coincides with point A_1 , while in Fig. 3b, the origin C is placed so that point A_1 moves along the y' -axis. For both robots, s is the distance between the parallel paths of points A_2 and A_3 , while in the Hephaist's alignment stage, h is the distance between the base x -axis and the path of point A_1 .

Referring to Fig. 3c, let points O_i be located at the vertices of an equilateral triangle fixed in the base. Let the origin O of the base frame coincide with O_1 , and let the base x -axis be along the line O_1O_2 . Let also the origin C be at the intersection of the three concurrent lines in the mobile platform, along which points A_i move. These three lines make up equal angles. Finally, the mobile y' -axis is chosen along the line A_1C .

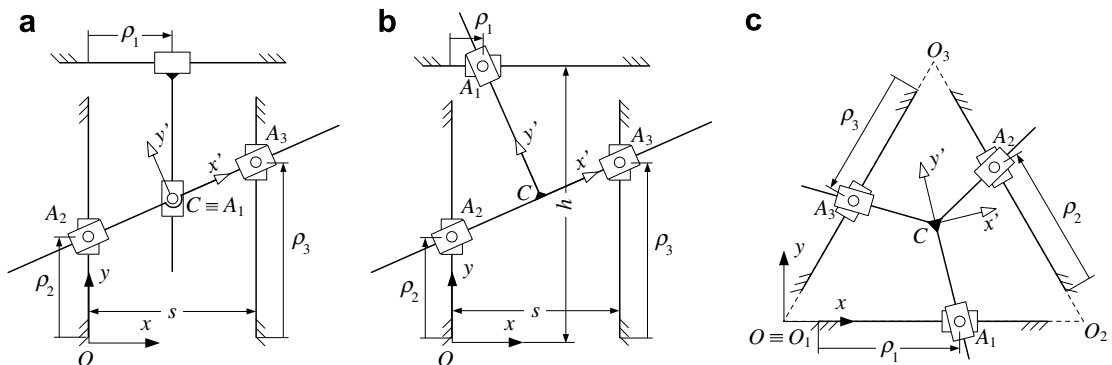


Fig. 3. Schematics of (a) PreXYT (patent pending), (b) Hephaist's parallel robot and (c) the Star-Triangle parallel robot.

Let ρ_i be the active-joint variables representing directed distances, defined as follows. For PreXYT and Hephaist's alignment stage (Fig. 3a and b), ρ_1 is the directed distance from the base y -axis to point A_1 , while ρ_2 and ρ_3 are the directed distances from the base x -axis to points A_2 and A_3 , respectively. Finally, for the Star-Triangle robot (Fig. 3c), ρ_i is the directed distance from O_i to A_i minus a constant positive offset d . Indeed, in the Start-Triangle robot, no mechanical design would allow point A_i to reach point O_i .

3.1. PreXYT

Given the active-joint variables, it is straightforward to uniquely define the position and orientation of the mobile platform. The orientation angle is easily obtained as

$$\phi = \tan^{-1} \left(\frac{\rho_3 - \rho_2}{s} \right), \quad (1)$$

while the position of the mobile platform is given by

$$x = \rho_1, \quad (2)$$

$$y = \rho_2 + \rho_1 \left(\frac{\rho_3 - \rho_2}{s} \right). \quad (3)$$

As one can observe, the direct kinematics of PreXYT are very simple and partially decoupled.

The inverse kinematic analysis is also trivial. Given the position and orientation of the mobile platform, the active-joint variables are obtained as

$$\rho_1 = x, \quad (4)$$

$$\rho_2 = y - x \tan \phi, \quad (5)$$

$$\rho_3 = y + (s - x) \tan \phi. \quad (6)$$

Obviously, PreXYT has no singularities (provided that s is non-zero).

3.2. Hephaist's parallel robot

Given the active-joint variables, it is simple to uniquely define the position and orientation of the mobile platform. The equation of the orientation angle is the same as Eq. (1). The position of the mobile platform is the intersection between line A_2A_3 and the line passing through point A_1 and normal to A_2A_3 . The resulting equations for x and y are therefore

$$x = \frac{s(\rho_1 s + (h - \rho_2)(\rho_3 - \rho_2))}{s^2 + (\rho_3 - \rho_2)^2}, \quad (7)$$

$$y = \frac{s^2 \rho_2 + h(\rho_3 - \rho_2)^2 + s \rho_1 (\rho_3 - \rho_2)}{s^2 + (\rho_3 - \rho_2)^2}. \quad (8)$$

As one can observe, the direct kinematics of Hephaist's parallel robot are more complex and highly coupled.

The inverse kinematics are easier to solve for. Given the position and orientation of the mobile platform, the active-joint variables are obtained as

$$\rho_1 = x - (h - y) \tan \phi, \quad (9)$$

$$\rho_2 = y - x \tan \phi, \quad (10)$$

$$\rho_3 = y + (s - x) \tan \phi. \quad (11)$$

Since Eqs. ((7)–(11)) are always defined (assuming $s \neq 0$), it is evident that this parallel robot too has no singularities. Note, that this is quite an advantage over most planar parallel robots, which have singularities.

3.3. Star-Triangle parallel robot

Given the active-joint variables, we are able to uniquely define the position and orientation of the mobile platform through this direct kinematic method used in [10]. Referring to Fig. 4, the position of C can be easily obtained through the following geometric construction based on the notion of the *first Fermat point*.

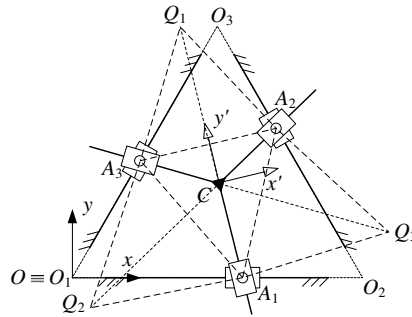


Fig. 4. Solving the direct kinematics of the Star-Triangle parallel robot.

Since in triangle $A_1A_2A_3$, none of the angles is greater than 120° (because points A_i cannot move outside the sides of triangle $O_1O_2O_3$), equilateral triangles are drawn outside of it. The outmost vertices of these triangles are denoted as Q_i (see Fig. 4). Then lines Q_iA_i make 120° angles and intersect at one point, the so-called first Fermat point. This point is the mobile frame's origin C .

While there is only solution for the position of the mobile platform, there are two possibilities for the orientation angle (ϕ and $\phi + 180^\circ$). Obviously, however, only one of these two solutions is feasible (the one for which $-90^\circ < \phi < 90^\circ$).

To find the coordinates of point C and the orientation angle θ , the following simple calculations need to be performed. Let \mathbf{q}_i denote the vector connecting point A_i to point Q_i , and $\mathbf{a}_i = [x_{A_i}, y_{A_i}]^T$ is the vector connecting point O to point A_i . Therefore, it can be easily shown that vector \mathbf{q}_i can be written as

$$\mathbf{q}_i \equiv \begin{bmatrix} x_{Q_i} \\ y_{Q_i} \end{bmatrix} = \frac{1}{2}(\mathbf{a}_j + \mathbf{a}_k) + \frac{\sqrt{3}}{2}\mathbf{E}(\mathbf{a}_j - \mathbf{a}_k), \tag{12}$$

where

$$\mathbf{E} = \begin{bmatrix} -1 & 0 \\ 0 & 1 \end{bmatrix}, \tag{13}$$

and $(i, j, k) = (1, 2, 3)$ or $(2, 3, 1)$ or $(3, 1, 2)$. Now, taking lines A_1Q_1 and A_2Q_2 for example, their intersection point is C and has the following coordinates:

$$x = \frac{(x_{A_1}y_{Q_1} - x_{Q_1}y_{A_1})(x_{A_2} - x_{Q_2}) - (x_{A_2}y_{Q_2} - x_{Q_2}y_{A_2})(x_{A_1} - x_{Q_1})}{(x_{A_1} - x_{Q_1})(y_{A_2} - y_{Q_2}) - (x_{A_2} - x_{Q_2})(y_{A_1} - y_{Q_1})}, \tag{14}$$

$$y = \frac{(x_{A_1}y_{Q_1} - x_{Q_1}y_{A_1})(y_{A_2} - y_{Q_2}) - (x_{A_2}y_{Q_2} - x_{Q_2}y_{A_2})(y_{A_1} - y_{Q_1})}{(x_{A_1} - x_{Q_1})(y_{A_2} - y_{Q_2}) - (x_{A_2} - x_{Q_2})(y_{A_1} - y_{Q_1})}. \tag{15}$$

The orientation of the mobile platform can be found by measuring the angle between line A_1C and the base y -axis

$$\phi = a \tan 2(y - y_{A_1}, x - x_{A_1}). \tag{16}$$

The inverse kinematics of this device is also easily solved for. Let $\mathbf{c} = [x, y]^T$ be the vector connecting the base origin O to the mobile frame origin C , \mathbf{b}_i be the unit length along O_iA_i and \mathbf{p}_i be the unit length along CA_i . Then, it can be easily shown that

$$\rho_i = \frac{\mathbf{b}_i^T \mathbf{E}(\mathbf{o}_i - \mathbf{c})}{\mathbf{b}_i^T \mathbf{E} \mathbf{p}_i} - d, \tag{17}$$

where d is the offset between the vertices of triangle $O_1O_2O_3$ and the initial positions of the corresponding linear actuators (see Fig. 3c).

4. Constant-orientation workspace analysis

There exists a simple geometric method for computing the constant-orientation (position) workspace of planar parallel robots [9]. Although, calculating the constant-orientation workspace for the three robots is not necessary for computing the accuracy of these robots, this workspace analysis shows that there is no simple relationship between accuracy and workspace shape and dimensions.

To allow for fair comparison, it will be assumed that the only limits restraining the workspace of the robots are the actuator limits. Under these conditions, the constant-orientation workspaces for all three planar parallel robots can be easily obtained geometrically, as shown in Fig. 5, where the constant-orientation workspaces for a given orientation are shown as the hatched regions.

From here, it is obvious that the constant-orientation workspace of PreXYT is greater than the constant-orientation workspace of Hephaist's robot, for any non-zero orientation. Furthermore, the constant-orientation workspace of PreXYT is always centered between actuators 2 and 3, while the location of the constant-orientation workspace of Hephaist's robot is hugely varying. This means that the region in which each point is accessible with at least one orientation in a given range, $\phi \in [-\phi_{\max}, \phi_{\max}]$, is much larger for PreXYT. However, the so-called maximal workspace (the set of all attainable positions) is much greater for the Hephaist's parallel robot.

Unfortunately, Fig. 5c does not show clearly whether the constant-orientation workspace of the Star-Triangle parallel robot is larger than that for the other two robots, because the orientation is not the same, nor are the limits of the actuators. In fact, for the zero orientation, the constant-orientation workspace of PreXYT is larger than that of the Star-Triangle parallel robot, but beyond some orientation angle, the situation is reverse. However, it is clear that the maximal workspace of the Star-Triangle parallel robot is greater than that of PreXYT (which is a square whose side is the actuators travel).

Intuitively, the larger is the maximal workspace of a robot, the smaller is its positioning accuracy. But if only maximum position errors are considered (as done in this paper), then it is not the area of the maximal workspace that defines accuracy but its extreme dimensions, as it will be seen in the next section.

5. Error analysis

For comparison reasons, it will be considered that all three parallel robots use the same actuators, whose stroke is 500 mm. Let $\varepsilon = 0.05$ mm be the accuracy of these actuators, meaning that if the nominal value of active-variable i is ρ_i , then its real value is somewhere in the range $[\rho_i - \varepsilon, \rho_i + \varepsilon]$. Let also the offset d for the Star-Triangle parallel robot be 100 mm. Based on these assumptions, it will now be shown that the maximum orientation and position errors can be found analytically using a simple geometric method.

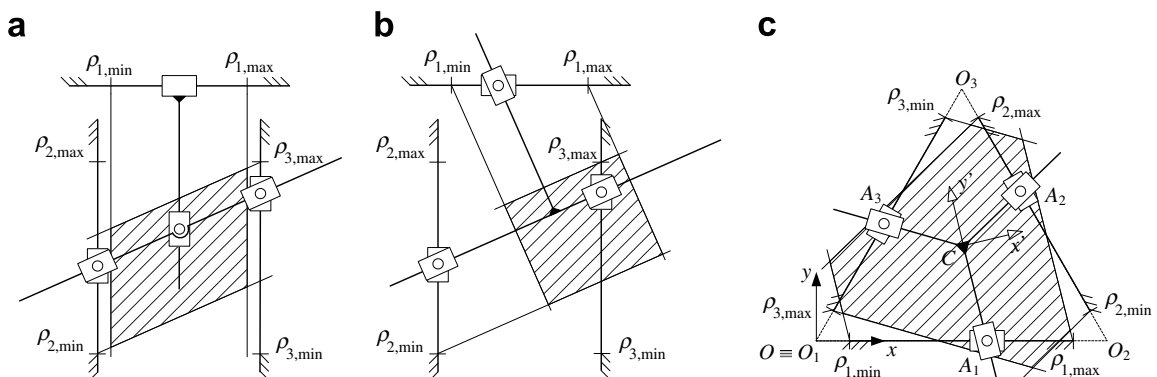


Fig. 5. Constant-orientation workspace for (a) PreXYT, (b) Hephaist's parallel robot and (c) the Star-Triangle parallel robot.

5.1. PreXYT

5.1.1. Maximum orientation error

Referring to Fig. 6a, it is obvious that the maximum orientation error does not depend on the nominal position of the mobile platform and occurs when actuators 2 and 3 are at $\rho_2 \pm \varepsilon$ and $\rho_3 \mp \varepsilon$, respectively (depending on the sign of the nominal orientation angle, it will be one of the two combinations). To solve analytically for the orientation error, a simple system of similar right triangles should be analyzed. Skipping the details, it can be shown that the maximum orientation angle is

$$\sigma_{\max} = \sin^{-1} \left(\frac{2\varepsilon \cos \phi}{\sqrt{s^2 + (s \tan \phi - 2\varepsilon)^2}} \right), \tag{18}$$

where ϕ is the nominal orientation angle. Fig. 7 shows a plot of the maximum orientation error of PreXYT as a function of nominal orientation. Obviously, it shows clearly that when ϕ increases, σ_{\max} decreases.

5.1.2. Maximum position error

Referring again to Fig. 6a, the hatched area is the maximal workspace for the considered ranges of the active-joint variables: $[\rho_i - \varepsilon, \rho_i + \varepsilon]$. Indeed, this is the region where point C can be located. Its geometric computation [9] is fairly simple for 3-DOF parallel robots whose legs have two prismatic joints and one revolute joint. The boundaries of the maximal workspace are the curves described by point C, when two actuators are at a limit. Note that for a general 3-DOF planar parallel robot, the boundaries of the maximal workspace may also include the curves for which a leg is at a singularity, which complicates the computation.

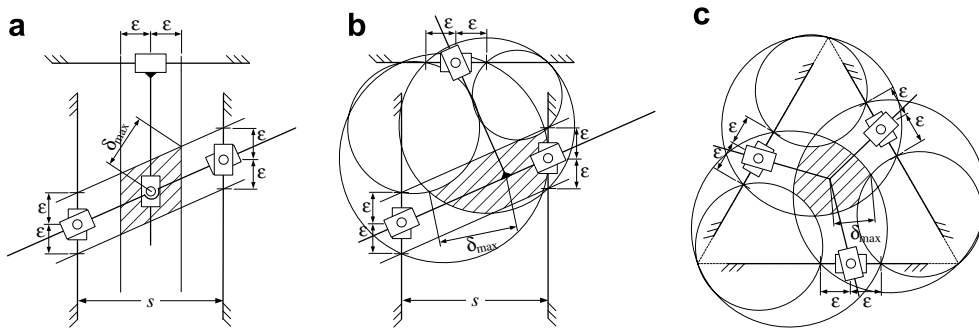


Fig. 6. Obtaining the maximum position error for (a) PreXYT, (b) Hephaist's parallel robot and (c) the Star-Triangle parallel robot.

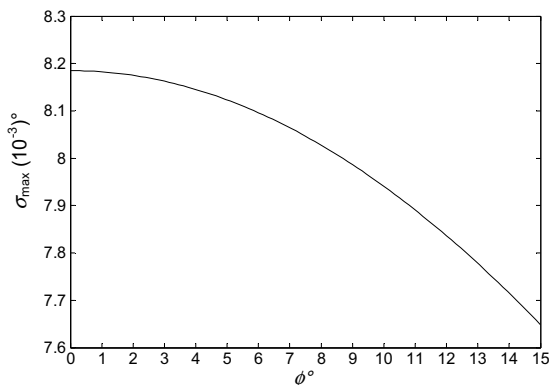


Fig. 7. Maximum orientation error as function of the nominal orientation angle for PreXYT.

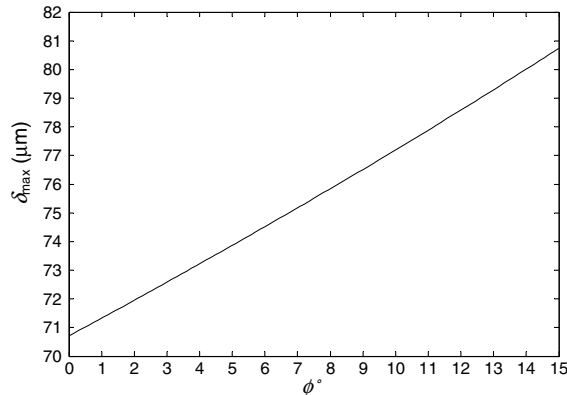


Fig. 8. Maximum position error as function of the nominal orientation angle for PreXYT.

Fortunately, however, none of the legs of all three parallel robots considered in this paper can be singular (without disassembling the robot).

To find the maximum position error, the maximum distance between the nominal position and the boundary of the maximum workspace should be found. This would be very difficult to do analytically for a general 3-DOF planar parallel robot, where the boundaries of the maximal workspace could be segments of ellipses or even sextics. However, for 3-DOF planar parallel robots whose legs have two prismatic joints and one revolute joint, the boundaries are usually circles (or even lines). And since the centers of these circles are obviously outside the maximal workspace (ε is very small compared to the actuators' stroke), the maximum position error occurs at one of the corners of the maximal workspace, i.e., when three actuators are at a limit. Therefore, only eight possibilities (eight corners) should be checked for each nominal position and orientation of the mobile platform.

For PreXYT, however, the maximal workspace is a parallelogram, and the maximum position error δ_{\max} is half its larger diagonal. Therefore, the following simple equation holds for PreXYT's maximum position error:

$$\delta_{\max} = \varepsilon \sqrt{1 + (1 + \tan \phi)^2}. \quad (19)$$

Note that PreXYT's maximum position error does not depend on the dimensions of the robot (the actuators' stroke and the distance s). A plot of this error as a function of ϕ is shown in Fig. 8.

5.2. Hephaist's parallel robot

5.2.1. Maximum orientation error

The analytic expression for the maximum orientation angle of Hephaist's parallel robot is obviously the same as the one for PreXYT, i.e., Eq. (18).

5.2.2. Maximum position error

The boundaries of the maximal workspace of Hephaist's parallel robot are arcs from four circles and segments from two lines (Fig. 6b). It can be observed that the maximum position error occurs when a maximum orientation error is present. Therefore, it is easy to see that only two configurations need to be tested to find the maximum position error: $\rho_1 - \varepsilon, \rho_2 + \varepsilon, \rho_3 - \varepsilon$ and $\rho_1 + \varepsilon, \rho_2 - \varepsilon, \rho_3 + \varepsilon$. Upon further analysis it was determined that if ϕ is positive, then the maximum position error occurs at σ_{\max} and $\rho_1 - \varepsilon$, otherwise the maximum position error occurs at σ_{\max} and $\rho_1 + \varepsilon$. Essentially, only one computation is needed to find the maximum position error of Hephaist's parallel robot for a given nominal position and orientation of the mobile platform.

Though an analytic expression for this maximum position error can be found easily, it will not be derived here. For a given nominal position and orientation, one need only to solve the direct kinematics for the right

combination of active-joint variables and calculate the distance between the nominal position and the new position. Using this procedure, a contour plot for the maximum positional error versus nominal position and for two given constant-orientations can be obtained (Fig. 9).

Fig. 9 clearly shows that as the mobile platform Hephaist’s parallel robot moves away from its maximum height, the maximum position error increases significantly. It is also evident that, overall, Hephaist’s parallel robot has a larger maximum position error than PreXYT.

5.3. Star-Triangle parallel robot

5.3.1. Maximum orientation error

Intuitively, the maximum orientation error occurs for $\rho_1 - \varepsilon, \rho_2 - \varepsilon, \rho_3 - \varepsilon$ or for $\rho_1 + \varepsilon, \rho_2 + \varepsilon, \rho_3 + \varepsilon$. Further inspection reveals that the maximum orientation error occurs for $\rho_1 - \varepsilon, \rho_2 - \varepsilon, \rho_3 - \varepsilon$, if $\phi \geq 0$, and for $\rho_1 + \varepsilon, \rho_2 + \varepsilon, \rho_3 + \varepsilon$, if $\phi \leq 0$.

Numerical analysis shows that within the workspace of the Star-Triangle parallel robot, the maximum orientation error is nearly the same, for any nominal position and orientation. Therefore, instead of showing a contour plot, or even a curve, only the mean value and the variance are given here for the maximum orientation error:

- $(\sigma_{\max})_{\text{mean}} = 14.177^\circ \times 10^{-3}$ and $(\sigma_{\max})_{\text{var}} = 9.71^\circ \times 10^{-27}$ for $\phi = 0^\circ$ and
- $(\sigma_{\max})_{\text{mean}} = 13.228^\circ \times 10^{-3}$ and $(\sigma_{\max})_{\text{var}} = 6.86^\circ \times 10^{-27}$ for $\phi = 15^\circ$.

Note that it is quite possible that the maximum orientation error is only a function of the nominal orientation angle ϕ , which would explain the virtually zero variance. Further analysis is needed to verify this interesting hypothesis, which would simplify enormously the computation of the maximum orientation angle.

It should be noted that the maximum orientation error for the Star-Triangle parallel robot is almost double the maximum orientation error of the other two parallel robots.

5.3.2. Maximum position error

As already mentioned, the maximum position error would occur when all actuators are at extreme positions (the corners of the maximal workspace, as shown in Fig. 6c). While probably there might be a way to discard some of the eight possible configurations, one can simply test all of them, without much worrying about computation time. Indeed, for each of the eight configurations, the corresponding position is obtained through the trivial direct kinematic Eqs. (14) and (15). Then the distance between this position and the nominal position is calculated, and the greatest of all eight distances is the maximum position error.

The contour plots for the maximum position error of the Star-Triangle robot (Fig. 10) clearly show that its average maximum position error is similar to that of PreXYT. This, however, is not what the dexterity plots in Fig. 1 suggest, which illustrates how dexterity is inadequate as a measure for accuracy.

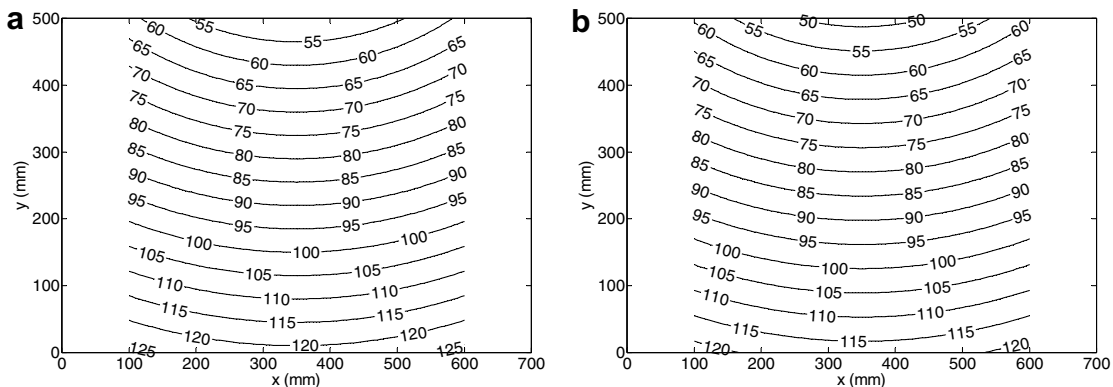


Fig. 9. Contour plots of the maximum position error (in μm) of Hephaist’s parallel robot for (a) $\phi = 0^\circ$ and (b) $\phi = 15^\circ$.

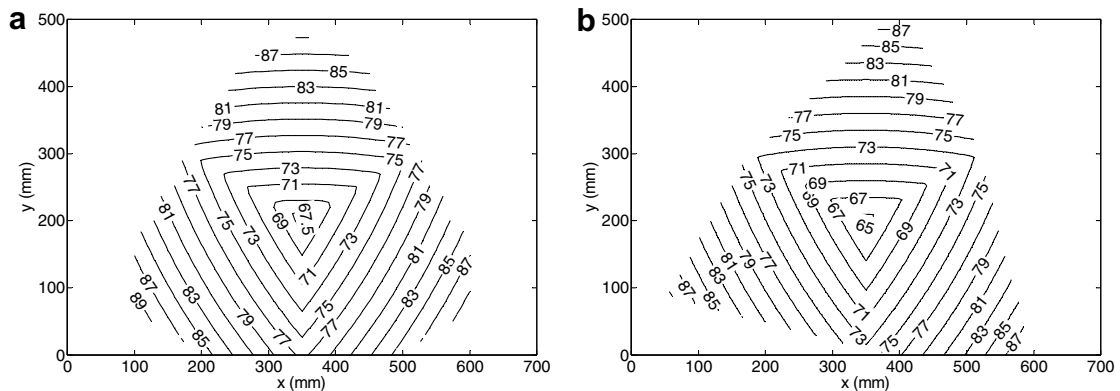


Fig. 10. Contour plots of the maximum position error (in μm) of the Star-Triangle parallel robot for (a) $\phi = 0^\circ$ and (b) $\phi = 15^\circ$.

Clearly, a more detailed comparison should be based on the mean value and variance of the maximum positioning and maximum orientation angles, over a specific workspace. Since these devices are most probably aimed at wafer alignment, such a workspace may be a circular area of diameter 300 mm in which any orientation in the range $\pm 5^\circ$ is possible. However, this is not the subject of this paper and will not be presented here.

6. Conclusion

This paper is in direct response to the failure of classical accuracy indices, such as the various local dexterity indices, in dealing with parallel robots with translational and orientational degrees of freedom, in the context of optimum design or comparison. Instead of using non-physical notions such as dexterity, the authors propose a simple geometric approach to determining the exact maximum position error and maximum orientation angle caused by actuator inaccuracies, at a given nominal position and orientation. Obviously, this method can also provide the maximum linear velocity and the maximum rotational velocity.

This approach works only for simple three-degree-of-freedom planar fully-parallel robots with no singularities. However, such robots are certainly the best candidate for micro-positioning and alignment. The authors illustrate the proposed geometric approach to three particular designs, one of which is commercially available. A simple comparison reveals major disadvantages for the commercially available design.

Acknowledgements

The authors would like to acknowledge the financial support of the Natural Sciences and Engineering Research Council of Canada (NSERC) and the Fonds Québécois de la recherche sur la nature et les technologies (FQRNT).

References

- [1] J.-P. Merlet, Jacobian, manipulability, condition number, and accuracy of parallel robots, *Journal of Mechanical Design* 128 (2006) 199–205.
- [2] C. Gosselin, The optimum design of robotic robots using dexterity indices, *Robotics and Autonomous systems* 9 (1992) 213–226.
- [3] C. Gosselin, J. Angeles, A global performance index for the kinematic optimization of robotic manipulators, *Journal of Mechanical Design* 113 (3) (1991) 220–226.
- [4] A. Yu, I.A. Bonev, P.J. Zsombor-Murray, New XY-Theta precision table with partially decoupled parallel kinematics, in: *International Symposium on Industrial Electronics*, Montreal, Canada, 2006.
- [5] J.-P. Merlet, D. Daney, Dimensional synthesis of parallel robots with a guaranteed given accuracy over a specific workspace, in: *IEEE International Conference on Robotics and Automation*, Barcelona, Spain, 2005.
- [6] S. Ronchi, O. Company, F. Pierrot, A. Fournier, PRP planar parallel mechanism in configurations improving displacement resolution, in: *Proceedings of the 1st International Conference on Positioning Technology*, Hamamatsu, Japan, June 9–11, 2004.

- [7] M.H.R. Daniali, P. Zsombor-Murray, J. Angeles, in: J. Angeles et al. (Eds.), *Computational Kinematics*, Kluwer Academic Publishers, 1993, pp. 153–164.
- [8] S. Briot, I.A. Bonev, Accuracy analysis of 3-DOF planar parallel robots, *Mechanism and Machine Theory*, accepted for publication.
- [9] J.-P. Merlet, C.M. Gosselin, N. Mouly, Workspaces of planar parallel manipulators, *Mechanisms and Machine Theory* 33 (1998) 7–19.
- [10] I.A. Bonev, A. Yu, P. Zsombor-Murray, XY-Theta positioning table with parallel kinematics and unlimited theta rotation, *International Symposium on Industrial Electronics*, Montreal, Canada, 2006.